



## **GAS LEAKAGE RATE THROUGH REINFORCED CONCRETE SHEAR WALLS: NUMERICAL STUDY**

**Ting WANG<sup>1</sup>, Tara C. HUTCHINSON<sup>1</sup>, Charles H. HAMILTON, Gerard C. PARDOEN<sup>1</sup>, and Michael W. SALMON<sup>2</sup>**

### **SUMMARY**

Unlined reinforced concrete (RC) shear walls are often used by the U.S. Department of Energy to house radioactive materials, thus providing a 'tertiary barrier'. Upon lateral earthquake loading, these stiff structural members are susceptible to large tensile and shear forces along their base and diagonal planes, where cracks can develop. Following an earthquake, dangerous gases (contained within the tertiary barrier) may leak into the environment through the cracks, lifting contamination to unsafe levels. The gas leakage rate through the damaged wall is therefore of primary concern.

In this research, the primary objective is to develop a methodology to analytically predict the leakage rate of gas through RC shear walls, when subjected to a broad range of lateral demands up to and beyond their normal design basis. This methodology includes two parallel and correlated approaches; experimental and analytical research. In each of the approaches, two relations being investigated are 1) damage vs. lateral load, and 2) gas leakage rate vs. damage. The relation between damage and lateral load is obtained by loading model specimens to a certain demand level, either physically or using finite element models. Gas leakage rate at different damage levels is measured using leakage rate tests in the experiment research, or numerically predicted by flow rate analysis in the analytical research. The experimental research program is described in detail in a companion paper [5], while this paper focuses on the methodology used in the analytical research.

Based on careful comparison between numerical and experimental lateral load-deformation behaviors, a finite element model of the specimen, built in a commercial package – MSC.Marc, is developed to capture the crack characteristics under prescribed lateral demands. By applying the available leakage rate estimation formulas in the literature to the numerically determined crack patterns on the specimen, leakage rates at different damage levels can be predicted. By comparing the predicted leakage rates with results obtained from the physical leakage rate experiments, the estimation formula most suitable for this case can be selected. Furthermore, the relation between the gas leakage rate and the shear wall lateral drift ratio or normalized lateral load is then established numerically.

---

<sup>1</sup> Doctoral Candidate, Asst. Professor, Post-doctoral Research Fellow and Lecturer, and Professor, respectively. Dept. of Civil and Environmental Engineering, University of California, Irvine, 92697-2175.

<sup>2</sup> Civil/Structural/Architectural Team Leader, Facilities and Waste Operations, Design Engineering, Los Alamos National Laboratory, MS 702 Los Alamos, NM 87545

## INTRODUCTION

There is an abundance of unlined RC shear wall type structures in the U.S. Department of Energy complex. Many of these structures serve as 'tertiary boundaries' to house radioactive materials, which may be dispersed through the air in an unanticipated event. Under normal operating conditions, the ventilation system for such facilities provides a negative pressure gradient to prevent unfiltered air leakage from the building. However, if an earthquake beyond the design basis event occurs, both the shear wall structure and the facility may be damaged. Normal or extreme wind loading on the building will result in regions where the external pressure is less than the internal pressure, which may allow air leakage out of the structure. The speed at which the hazardous gas leaks into the environment, and as a result, the needed time to repair these structures in order to control the contamination within a safe level, are therefore of primary concern.

### **Previous Studies Investigating Leakage Rate through RC Members**

Previous investigations into the leakage rate of gas have indicated its dependence upon many factors, including, the property of the gas itself, the media property through which the gas passes, and the pressure gradient. Among these factors, the media property itself potentially plays the most significant role in the final rate of gas leakage. For example, the leakage rate of air can increase by a factor of 40 once through shear cracks occur [3]. Because of this, it is reasonable to neglect the leakage rate through the undamaged concrete portion, for a damaged wall. Since the focus of this work is on RC shear walls subjected to lateral demands up to and beyond their normal design basis, it is assumed that the shear wall has already been damaged. Therefore, in this literature review, the identified leakage rate estimation formulas focus on those obtained from damaged concrete specimens.

Research on the leakage rate of gas through unlined concrete elements can be found in the literature as early as the 1970s. Buss [1] is perhaps identified as the first to examine the leakage of air specifically passing through concrete cracks. Numerous authors have since conducted experiments to determine the leakage rate of gas and derive leakage rate formulas describing the relation between the damage and the leak rates of gas (Rizkalla [13], Tinkler [16], Mayrhofer [6], Nagano [8], Suzuki [14, 15], Girrens [3], Okamoto [10], Greiner [4], and Riva [12]). These previous studies, as noted in Table 1, may be classified by the applied load conditions and the damage indicators used in the derived leakage formulation. Load conditions have incorporated tensile, shear and bending experiments, depending upon the predominant force (tensile, shear, or bending-induced forces) causing damage to the concrete member. Damage indicators may be classified as either a global indicator or a local indicator (crack characteristics). Global indicators include such things as, the global external force, global displacement, average stress, or average strain. Crack characteristics are local in nature, whereby the length, width and depth of the cracks are used in the formulation.

Studying the summary information provided in Table 1, several observations can be made. First, only a few researchers (Nagano [8], Girrens [3], and Okamoto [10]) conducted shear member tests. Of these previous studies where shear-dominated loading was applied, only the work of Nagano [8] considered crack characteristics in the formulation of leakage rate estimation. Although global indicators, such as the global deformation, are very convenient for practical applications, they are not directly related to the leakage rate. Given the same global indices, different specimen configurations, for example, the concrete strength, the reinforcement ratio, aspect ratio of the shear walls and loading conditions, will result in different leakage rates. Therefore, formulas using global indicators may only be applicable in select special cases, and are difficult to extend to more general situations. On the contrary, cracks are the direct cause of the leakage. Therefore characteristics such as the crack length, width and depth are reasonable selections to indicate the damage attained by RC members.

**Table 1. Previous studies on leakage rate through damaged concrete elements.**

	Load Condition			Damage Indicator	
	Tensile Test	Shear Test	Bending Test	Global indicator	Crack Characteristics
Rizkalla [13]	✓				✓
Tinkler [16]	✓				✓
Mayrhofer [6]			✓	✓	
Nagano [8]		✓		✓	✓
Girrens [3]		✓		✓	
Suzuki [14], [15]	✓				✓
Okamoto [10]		✓		✓	
Greiner [4]	✓				✓
Riva [12]	✓				

Second, most formulas using crack characteristics as the damage indicator, were derived from pure tensile tests. Tensile tests may be readily related to anticipate conditions within the vessels in nuclear power plants, where the high internal pressure causes membrane tensile stress in the container walls. Therefore, verification of the formulas obtained from tensile experiments warrants further study. Third, previous studies using crack characteristics as a damage indicator develop flow rate estimation formulas by physically measuring the crack patterns and the flow rate. Since there is no standard method to calculate crack patterns, these leakage rate formulas are difficult for practitioners to use in a realistic design situation. Among the studies cited above, Riva [12] is the only one to predict the leakage rate of gas using crack characteristics obtained from nonlinear finite element analyses results. The specimen in this study was subjected to pure tension along a single axis. However, it is unclear how results from this loading condition can be extrapolated to more complex loading conditions, for example where combined shear and bending occur.

### Scope of this Paper

The focus of this paper is to develop a methodology to analytically predict the leakage rate of gas through RC shear walls. Two parallel and correlated approaches are included in this research: experimental and analytical research. In each of the approaches, the two relations being investigated are: 1) damage vs. lateral load, and 2) gas leakage rate vs. damage. The relation between damage and lateral load is obtained by loading model specimens to a certain demand level, either physically or using finite element models. Gas leakage rate at different damage levels is measured using leakage rate tests in the experimental research program, or numerically predicted by flow rate analysis in the analytical research program. These experiments not only contribute additional results to a sparse available literature in this problem area, as well, they can be used to correlate and verify the numerical models to be established in the analytical research. The experimental research is described in detail in a companion paper [5], while this paper will focus on the methodology used in the analytical research.

## FINITE ELEMENT ANALYSIS

The purpose of the finite element analysis is to predict the damage level of the RC shear walls subjected to different lateral demands. Crack characteristics, such as the length, width and the depth of the cracks, are chosen as the damage indicator in the present study. These characteristics can be simulated using the strain field obtained from the finite element analysis, and subsequently are used to predict the flow rate through a specimen using flow rate estimation formulas available in the literature. In this sense, the crack characteristics play an important role in linking the finite element analysis and flow rate analysis. In the following paragraphs, the finite element model, analysis results, and the method to simulate the cracks will be discussed in detail.

## Finite Element Model

Of primary concern in capturing the local characteristics of the RC members of interest in this study, is providing a reasonable account for the cracks developed in the member. To consider the cracked behavior of RC members, two primary finite element methods that have been studied are the discrete crack model and the smeared crack model. The discrete crack model, proposed by Ngo [9], involves using a predefined discrete crack pattern on the model. This approach represents a crack as a geometric discontinuity by using interface elements. The smeared crack model, was introduced later, to investigate the response of gas cooled nuclear reactor vessels by Rashid [11], and Echeverria [2]. In this approach, the cracked material is regarded as a continuum with reduced stiffness properties, thus smearing the effect of local cracks within the region of interest. Since this method is easier to apply, without significant loss in accuracy, it is more commonly used in research. As the primary concern is the leakage rate of gas through the entire wall, rather than the propagation and local discreteness of cracks, the smeared crack model, is a reasonable approach in the present study.

In this work, the commercial finite element analysis code – MSC.Marc [7] is adopted, for two primary reasons. First, it provides a smeared crack approach to account for the cracking attained in RC members. As shown in Figure 1, a low-tension material model is available for capturing the constitutive behavior of concrete and specifically for estimating the cracked contribution to this behavior. Under uniaxial compression, defined input properties include such values as Young’s modulus  $E_c$ , uniaxial compressive strength  $f'_c$ , Poisson’s ratio  $\nu_c$ , and crushing strain  $\epsilon_{crush}$ . Tensile properties, such as the peak tensile strength  $f_t$ , softening modulus  $E_{so}$ , and shear retention can also be input as part of the cracking data. Second, a series of built-in rebar elements are available to directly model the effect of the reinforcement in RC members. This embedded rebar approach naturally captures the interaction between the concrete and steel. However, since the rebar elements share the same nodes and deformation with the concrete element, the bond-slip effect, which is important to RC members, cannot be simulated. However, in low aspect RC shear walls, the bond-slip effect does not play a major role; therefore, using this embedded rebar is reasonable in this study.

As illustrated in Figure 2, the RC material is modeled using filler elements embedded with rebar elements. Filler elements are regular 3D elements (element 7: 8-node solid elements), assigned with the concrete material property. Sharing the same nodes and same deformation with the filler elements, rebar elements (element 146: 8-node rebar elements) are defined by inputting the orientation, the area and the position of the reinforcement, to consider the effect of the reinforcement.

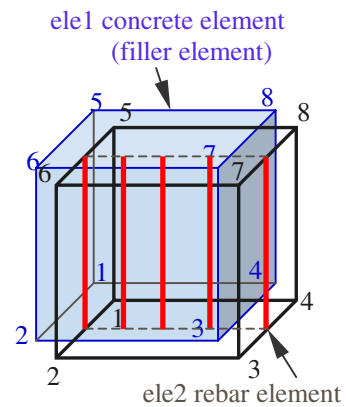
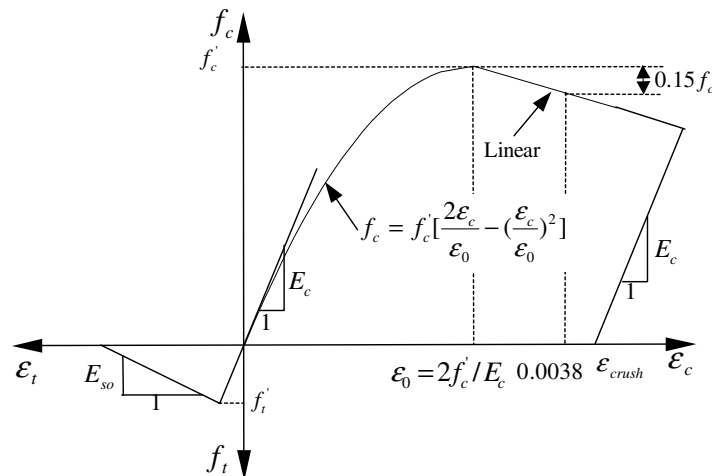


**Figure 1. Nonlinear material model of concrete. Figure 2. Rebar element embedded in filler element**

For this paper, a finite element model of the specimen described in the companion experimental paper [5] is constructed as shown in Figure 4. Elements are selected as 3 inches (7.6 cm) in each direction for convenience of modeling (as shown in Figure 3). At the same time, this matches the requirement that the element size of concrete elements should be at least four times the size of the coarse aggregate when concrete is considered as a homogeneous material. To represent the experimental boundary and loading conditions, the entire specimen is fixed at the bottom points, and subjected to evenly distributed monotonic surface loading at the top of the flange wall, as shown in Figure 4. The concrete model discussed above and shown in Figure 1 is used to represent the properties of concrete. A bi-linear elastic-plastic model is used to represent the properties of the reinforcing steel, where the Young's modulus  $E_s$ , Poisson's ratio  $\nu_s$ , yield strength  $f_y$ , ultimate strength  $f_u$ , and ultimate strain  $\epsilon_u$  (strain corresponding to the ultimate strength) are defined in the model. Input properties selected for these material models are listed in Table 2. Note the region of interest, through which the gas was passed in the experiment, is highlighted in Figures 3 and 4.

**Table 2 Selection of material properties.**

<i>Concrete</i>						
$E_c$	$\nu_c$	$f'_c$	$\epsilon_{crush}$	$f'_t$	$E_{so}$	Shear retention
$3 \times 10^6$ psi	0.2	4440 psi	0.008	266 psi	250000 psi	0.5
<i>Steel</i>						
	$E_s$	$\nu_s$	$f_y$	$f_u$	$\epsilon_u$	
Horizontal reinforcement	$2.9 \times 10^7$ psi	0.3	65300 psi	97200 psi	0.145	
Vertical reinforcement			85800 psi	122000 psi	0.113	
Starter reinforcement			73800 psi	97300 psi	0.120	

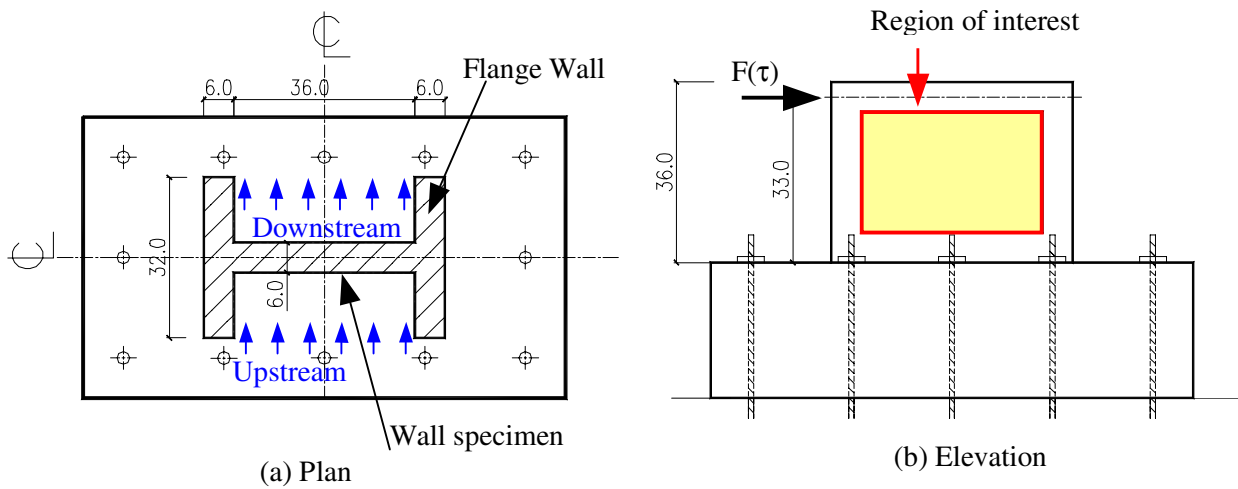


**Figure 3. Schematic of specimen (dimensions in inches).**

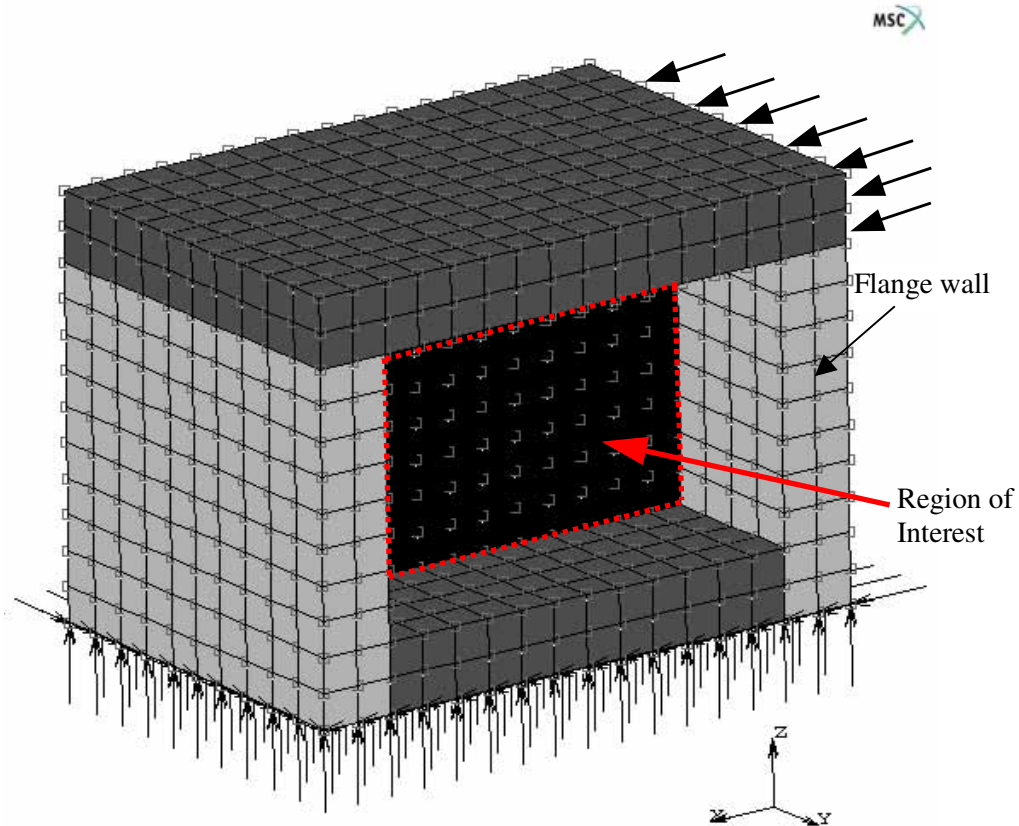


**Figure 4. 3D finite element model of specimen described in the companion paper [5].**

### **Analysis Results**

Nonlinear analysis of the specimen model described above is conducted using an incremental load control solution. Comparison of the global lateral load-displacement response obtained from the experiment and that from the finite element analysis are illustrated in Figure 5. Note that in the experimental program, three reversed cycles of lateral loading are applied, with incremental increases, defined as a percentage of the calculated nominal capacity of the specimen ( $\phi V_n = 163.5$  kips). For the purposes of simplicity, in the numerical model, monotonic loads are applied, with unloading at each target load value, based on the elastic stiffness of the member. Considering this approach, four points of interest are defined on the push portion of the load-displacement curve (denoted points 1-4 in Figure 5). The cracking strain  $\epsilon_i$  at the end of the two loading levels (points 1 and 3) is illustrated in Figures 6 and 7. From these two figures, the cracking strain is observed to mainly distribute along the diagonal direction of the member, and also occur below the main diagonal line. However, almost no cracking strain was observed above the diagonal line. These properties are consistent with the phenomena observed in the experiment. Under the load level of  $0.75\phi V_n$ , the maximum cracking strain is  $7.8 \times 10^{-4}$ , and it increases to  $1.3 \times 10^{-3}$  under the load of  $\phi V_n$ .

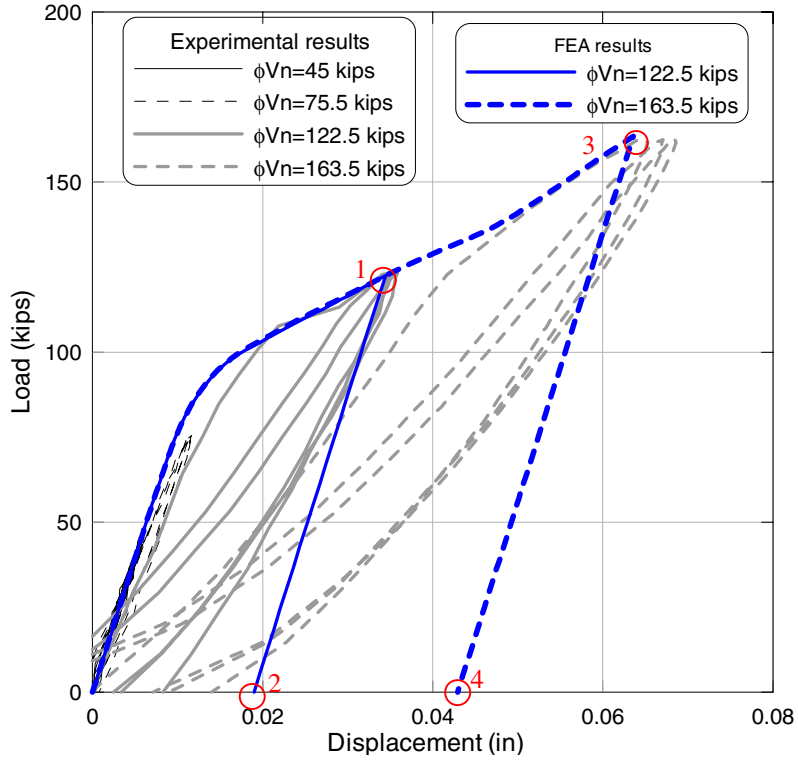


Figure 5. Comparison of experimental and finite element results.

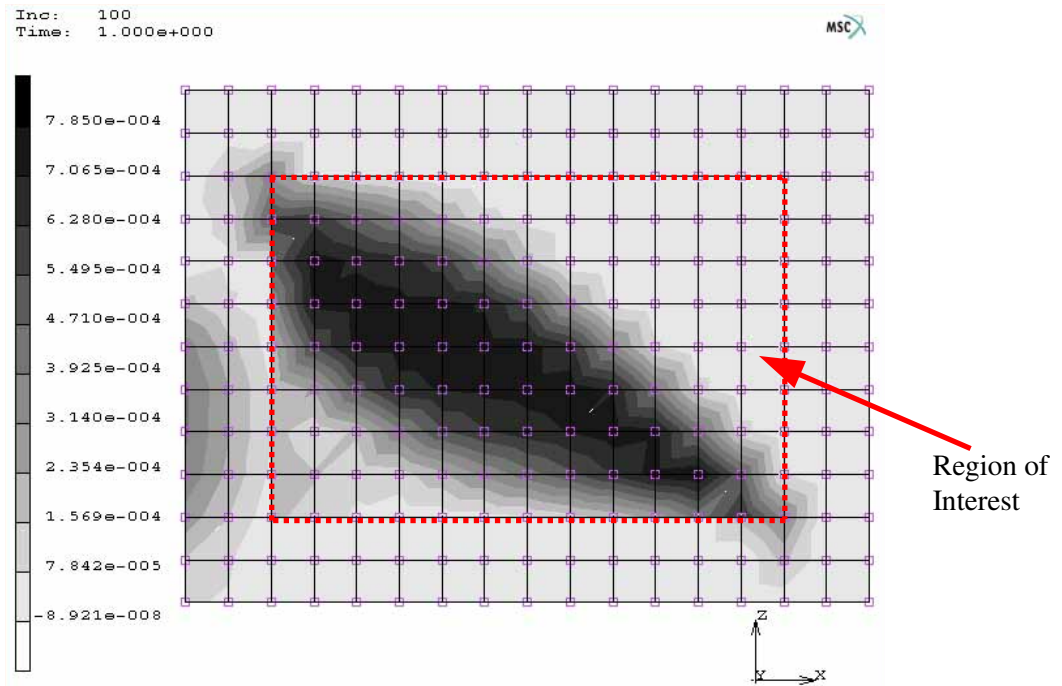


Figure 6. Cracking strain  $\epsilon_t$  distribution at  $0.75\phi V_n = 122.5$  kips (point 1 in Figure 5).

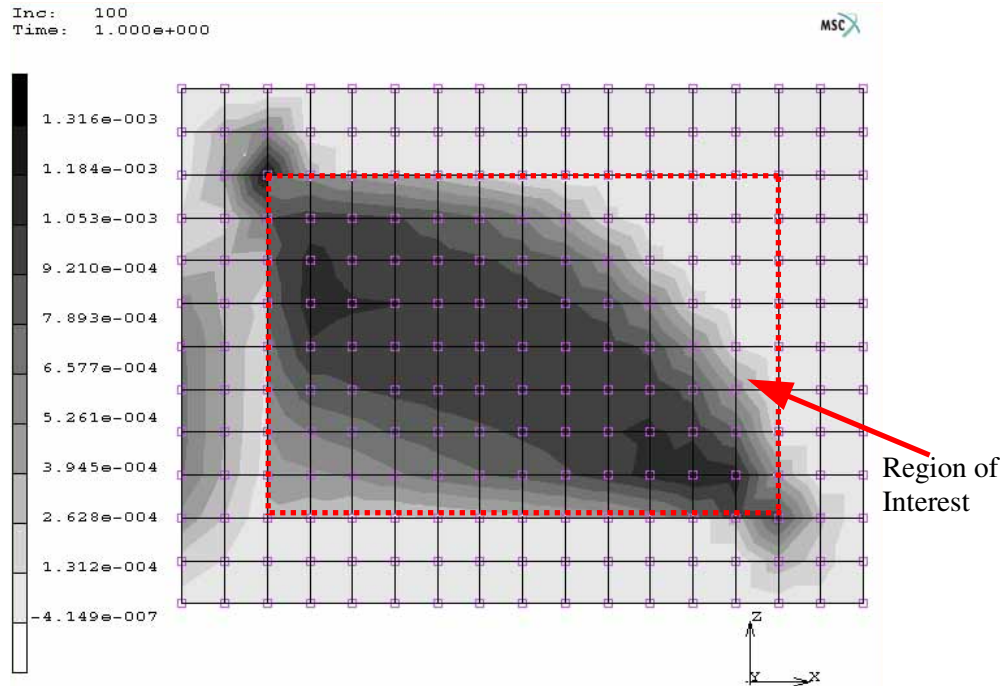
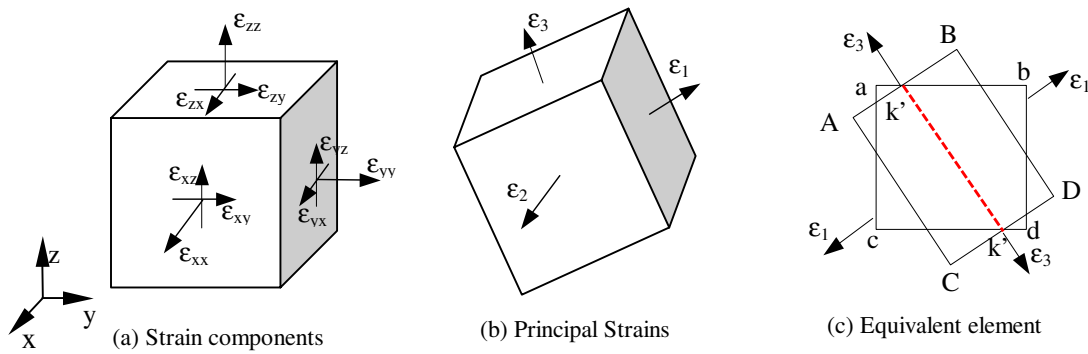


Figure 7. Cracking strain  $\epsilon_t$  distribution at  $\phi V_n = 163.5$  kips (point 3 in Figure 5).

### Estimation of Crack Distribution and Properties

The strain field within the concrete (filler) elements can be obtained from the finite element analysis results, which is presented by six strain components at each of the Gaussian points. Since the element is only 3 inches (7.6cm) in each direction, it is reasonable to simplify each of the elements with the same strain components [shown as Figure 8(a)]. The strain at the center of the element is used to represent the strain of the entire element in this estimation. When the strain components at the center of the element are obtained, three principal strains and corresponding directions for each element can be obtained, as illustrated in Figure 8(b). Since the shear wall is subjected to in-plane forces, most elements are in a plane stress condition, with the exception of those constrained by boundary elements (such as the flange wall). Therefore, the second principal strain  $\epsilon_2$ , which will occur in the direction perpendicular to the shear wall thickness, will have a very small value. In this case,  $\epsilon_2$  can be ignored in the crack estimation. Under two principal strains  $\epsilon_1$  and  $\epsilon_3$ , the crack ( $k'k'$ ) is assumed to appear perpendicular to  $\epsilon_1$ , or along the direction of  $\epsilon_3$ , passing the center of the element, as shown in Figure 8(c). An equivalent element ABCD may then be defined and used to calculate the length and width of the crack. AC and BD are parallel to  $\epsilon_3$ , with a length equal to  $k'k'$ . AB and CD are parallel to  $\epsilon_1$ , with their length selected such that the equivalent element ABCD has the same area with the original element abcd. To use this procedure with the finite element analysis results, the maximum principal strain ( $\epsilon_1$ ) is compared with the cracking strain ( $\epsilon_t'$ ), which corresponds to the cracking stress  $f_t$ . When  $(\epsilon_t' - \epsilon_1)$  is less than zero, the equivalent crack width is calculated by multiplying  $(\epsilon_t' - \epsilon_1)$  with the length of AB. The simulated crack distribution and widths on the specimen at  $0.75\phi V_n$  are shown in Figure 9. The number presented in each element is the crack width in inches.



**Figure 8. Estimation of crack properties using the calculated strain components.**

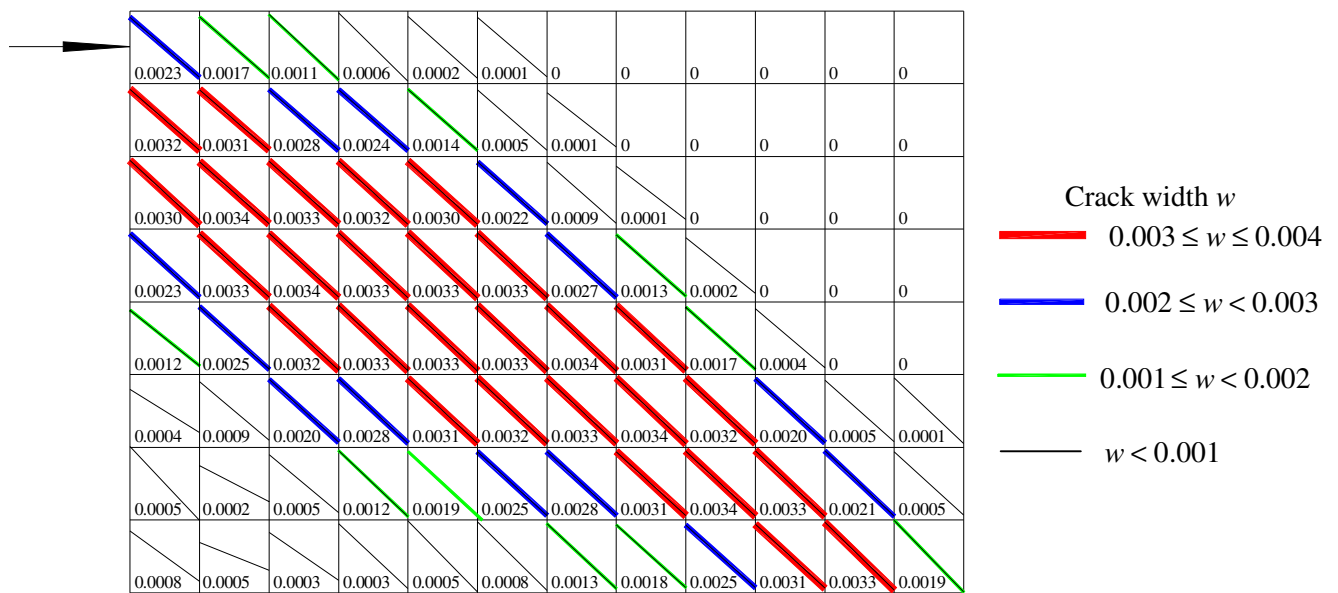


**Figure 9. Simulated crack width and direction at  $0.75\phi V_n$  (point 1 in Figure 4). (crack widths presented in inches, 1 inch = 25.4mm).**

### FLOW RATE ANALYSIS

Flow rate analysis is conducted to estimate the rate at which gas flows through the specimen. In this work, the simulated crack characteristics combined with select flow rate estimation formulas available from the literature are used to estimate the gas flow rate. In the following paragraphs, the selection of compatible flow rate formulas, the estimation methods, and the results specific to the specimen of interest in this study are presented in detail.

#### Selected Flow Rate Formulas

From the discussion in the previous studies, it is observed that only one formula (Nagano [8]) is available in the literature to describe the relation between the flow rate and crack characteristics through the shear walls. Since the cracks on shear walls are due to the stress of concrete in the diagonal direction larger than the tensile strength of concrete, three formulas describing the flow rate through tensile cracks are also selected as suitable for comparison in this study. Each of these is briefly described herein.

Rizkalla [13] tested eight reinforced concrete specimens subjected to tensile membrane forces and proposed a mathematical expression by assuming that the flow through a concrete crack may be idealized as a flow through a gap between two parallel plates, and considering the friction between flow and cracks from their test data. Nagano [8] used 2-dimensional Poiseuille's flow equation with no friction considered to estimate the flow rate of gas through shear cracks. Suzuki [15] investigated the gas leakage rate through cracks in both reinforced and unreinforced concrete tensile specimens with notches. They proposed two mathematic formulas to describe the relation between crack characteristics and flow rate. The first formula (here termed *Suzuki-1*) was based on the model that an isothermal compressible gas flows between two parallel plates, and the observation from the experiments that the production of the friction coefficient at the cracks and the flow rate changes linearly with the flow rate of the gas. The second formula (here termed *Suzuki-2*) used the Poiseuille's flow equation to describe the slow gas flowing through concrete cracks. The difference between this formula and that given by Nagano [8] is that Suzuki-2 used an empirical coefficient  $c(W)$  to consider the friction between flow and cracks. These four formulas are listed in Table 3.

**Table 3. Leakage rate estimation formulas available in literature.**

Reference	Expression	Parameters
Rizkalla et. al.(1984) [13]	$\frac{P_1^2 - P_2^2}{t} = \left( \frac{k^n}{2} \right) \left( \frac{\mu}{2} \right)^n \frac{(RT)^{n-1}}{W^3} \left  \frac{P_2 Q}{L} \right ^{2-n}$	$n = \frac{0.133}{W^{0.243}}, k = 2.907 \times 10^7 W^{1.284}$
Nagano et. al. (1989) [8]	$Q = LW^3 \frac{P_1 - P_2}{12\mu t}$	
Suzuki-1 et. al. (1992) [15]	$Q^2 = \frac{W^3 (P_1^2 - P_2^2)}{2\rho_0 P_0 t [\bar{a}(W) \frac{12\mu_0}{\rho_0 Q} + b(W)]}$	$\bar{a}(W) = 4.33 \times 10^{-5} / W^{1.5} + 1$ $b(W) = 3.41 \times 10^{-4} / W$
Suzuki-2 et. al. (1992) [15]	$Q = c(W) LW^3 \frac{P_1 - P_2}{\mu t}$	$c(W) = 15.3W + 7.56 \times 10^{-3}$

In Table 3,  $Q$  is the flow rate;  $P_1, P_2$  are the absolute upstream and downstream air pressure (as shown in Figure 3);  $T$  is the absolute temperature;  $R$  is the gas constant;  $\mu$  is the dynamic viscosity of air;  $\rho$  is the air density;  $L, W,$  and  $t$  are the length, width and depth of the cracks, respectively. The subscript 0 refers to the value under standard condition (1atm and 20°C).

### Estimation of the Flow Rate through RC Walls

Since these four formulas are derived from experiments of visible tensile cracks, further consideration is needed, as the crack widths in the present research are sometimes very small and may even be zero, as shown in Figure 9. The estimation formulations presented in Table 3 may not explicitly account for zero width cracks. Specifically, the limit state encountered at zero crack width ( $W=0$ ) using Rizkalla's and the Suzuki-1 formulas may be accounted for using an analytical approach for the zero limit estimation, e.g. applying L-Hospital's rule. In the present paper, however, this state is not considered, and rather the flow rate is only calculated where cracks have a width greater than 0, i.e., any flow through the predicted undamaged region of the wall is ignored. Figure 10 shows the relation between the flow rates of air through a crack with a width less than 0.001 in (0.025mm), using the formula by Rizkalla, and for a range of differential pressures [ $(P_1 - P_2) = 0.25 - 2.50$  psi]. It can be seen that it is reasonable to calculate the flow rate through a crack width, which is greater than  $4 \times 10^{-4}$  in (0.01mm) using this formula. It also makes sense that when differential pressure increases, the flow rate through a crack of a given width increases.

The flow rates of air through the simulated crack of each element in the specimen are calculated by one of the four methods listed above. Individual element flow is then summed together across the entire specimen region of interest to obtain its potential flow rate at different damage states. The four crack conditions, corresponding to the four points shown in Figure 5, which are related to the load of  $0.75\phi V_n$  (point 1) and  $\phi V_n$  (point 3), and the unloading from these respective points (points 2 and 4), are used. A comparison of experimental and analytical results is listed in Tables 4 and 5 (for points 2 and 4).

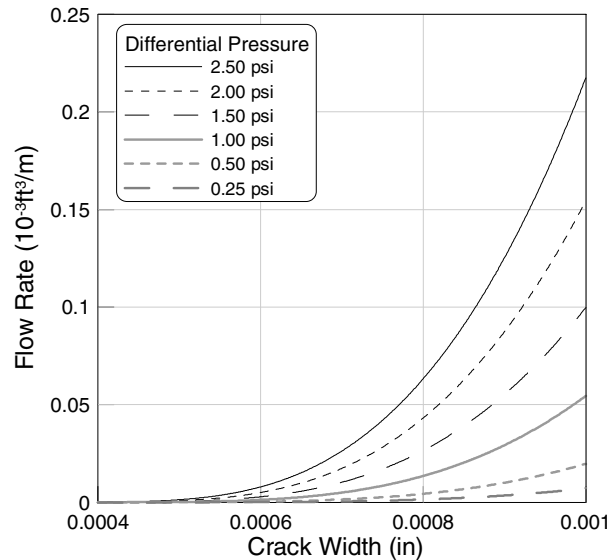


**Figure 10. Flow rate through cracks under different differential pressure (using Rizkalla’s formula).**

Results presented in Tables 4 and 5, as well as data calculated at points 1 and 3 on Figure 5, are also plotted in Figure 11. Each graph shows the ratio of the flow rate determined analytically (e.g.  $Q_{riz}$ ,  $Q_{nag}$ ,  $Q_{suz-1}$ ,  $Q_{suz-2}$ ) by one of four methods listed above to that obtained from the experiment, taken at different differential pressures, and corresponding to the 4 points in Figure 5. It should be noted that experimental flow measurements were only made after complete unloading of the specimen. Therefore, all references to  $Q_{exp}$  in Tables 4 and 5 refer to the unloaded condition. It can be seen that all results shown in Figure 11 are nearly horizontal, which indicates the ratio of analytical to experimental results is nearly constant with varying differential pressure. The maximum coefficient of variation *COV* among all the data for each method at each condition is 3%. This indicates that at the range of damage considered and differential pressure in the present research, the applied methodology can estimate the flow rate in a stable manner. From Figure 11, it is also noted that estimates of flow rate at points 1 and 3 are always higher than those obtained at points 2 and 4. While some visible cracks are still present at unloading, clearly larger cracking will be observed at peak loading, and the leakage rate formula are capturing this. At the same time, when using elastic response to simulate the unloading processes, the global displacement is still larger than that obtained from the experiment. Given that larger deformation generally implies larger local strain and larger cracks, the estimated flow rates at point 2 and 4 are also larger than experimental results.

Important to note from Figure 11 is that, among the four methods considered, Suzuki-1s’ formula provides the best estimation for each of the four conditions. In this case, the ratio between analytical and experimental results ranges from 1 – 8. Nagano’s formula resulted in the least favorable estimation, overestimating the experimental flow rates by as much as 300 times. The basic difference between Nagano’s formula and the other three formulas is that the Nagano derivation is based on the assumption that incompressible gas passes through smooth walls, therefore, no friction is considered in the flow rate

estimation formula. This can dramatically overestimate the leakage rate of gas, as was also observed by Riva [12]. The other three formulas consider the friction between the flow and the crack using experimental data, although based on different assumptions for the air flowing through the crack. Comparing the experiments conducted by Rizkalla and Suzuki, it is observed that the differential pressure was as high as 30 psi (0.207MPa) in Rizkalla's test. In Suzuki's test, especially for the second formula, the differential pressure is less than  $0.2 \times 10^5$  Pa (2.9 psi), which is about the same level as that in the present research. The similarity in differential pressures between Suzuki's tests and those modeled here, may account for the reason Suzuki's formulas provide the best estimate of flow rate.

**Table 4. Comparison of experimental and analytical results of the flow rate at point 2.**

$P_1$ (Psia)	$P_2$ (Psia)	$T$ (°F)	$Q_{exp}$ ( $10^{-3}$ ft <sup>3</sup> /min)	$Q_{Riz}$ ( $10^{-3}$ ft <sup>3</sup> /min)	$\frac{Q_{Riz}}{Q_{exp}}$	$Q_{Nag}$ ( $10^{-3}$ ft <sup>3</sup> /min)	$\frac{Q_{Nag}}{Q_{exp}}$	$Q_{Suz-1}$ ( $10^{-3}$ ft <sup>3</sup> /min)	$\frac{Q_{Suz-1}}{Q_{exp}}$	$Q_{Suz-2}$ ( $10^{-3}$ ft <sup>3</sup> /min)	$\frac{Q_{Suz-2}}{Q_{exp}}$
16.97	14.83	64.6	64.7	765.7	11.8	5093.8	78.7	72.0	1.1	526.9	8.1
15.66	14.81	63.2	26.3	285.5	10.9	2027.5	77.1	27.4	1.0	209.7	8.0
15.09	14.82	63.2	8.29	86.6	10.5	644.0	77.7	8.5	1.0	66.6	8.0
15.35	14.85	62.5	16.15	164.1	10.2	1194.0	73.9	15.9	1.0	123.5	7.7
16.22	14.84	64.4	43.8	476.5	10.9	3285.8	75.0	45.4	1.0	339.8	7.8

**Table 5. Comparison of experimental and analytical results of the flow rate at point 4.**

$P_1$ (Psia)	$P_2$ (Psia)	$T$ (°F)	$Q_{exp}$ ( $10^{-3}$ ft <sup>3</sup> /min)	$Q_{Riz}$ ( $10^{-3}$ ft <sup>3</sup> /min)	$\frac{Q_{Riz}}{Q_{exp}}$	$Q_{Nag}$ ( $10^{-3}$ ft <sup>3</sup> /min)	$\frac{Q_{Nag}}{Q_{exp}}$	$Q_{Suz-1}$ ( $10^{-3}$ ft <sup>3</sup> /min)	$\frac{Q_{Suz-1}}{Q_{exp}}$	$Q_{Suz-2}$ ( $10^{-3}$ ft <sup>3</sup> /min)	$\frac{Q_{Suz-2}}{Q_{exp}}$
16.68	14.78	69	108.34	3023.3	27.9	22089.3	203.9	536.5	5.0	2411.3	22.3
15.80	14.78	67.8	60.54	1641.0	27.1	11879.9	196.2	280.6	4.6	1296.8	21.4
15.58	14.77	68.8	47.22	1310.9	27.8	9419.9	199.5	221.9	4.7	1028.3	21.8
15.31	14.78	66.6	31.3	874.2	27.9	6184.1	197.6	143.5	4.6	675	21.6

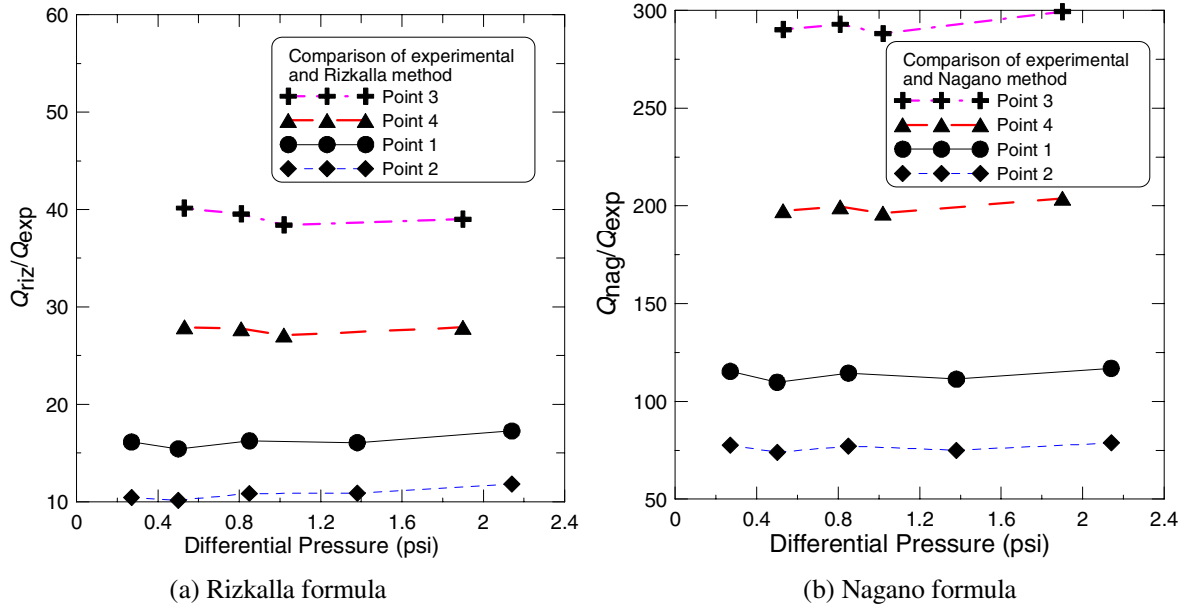


**Figure 11. Comparison of experimental and analytical results of flow rate prediction.**

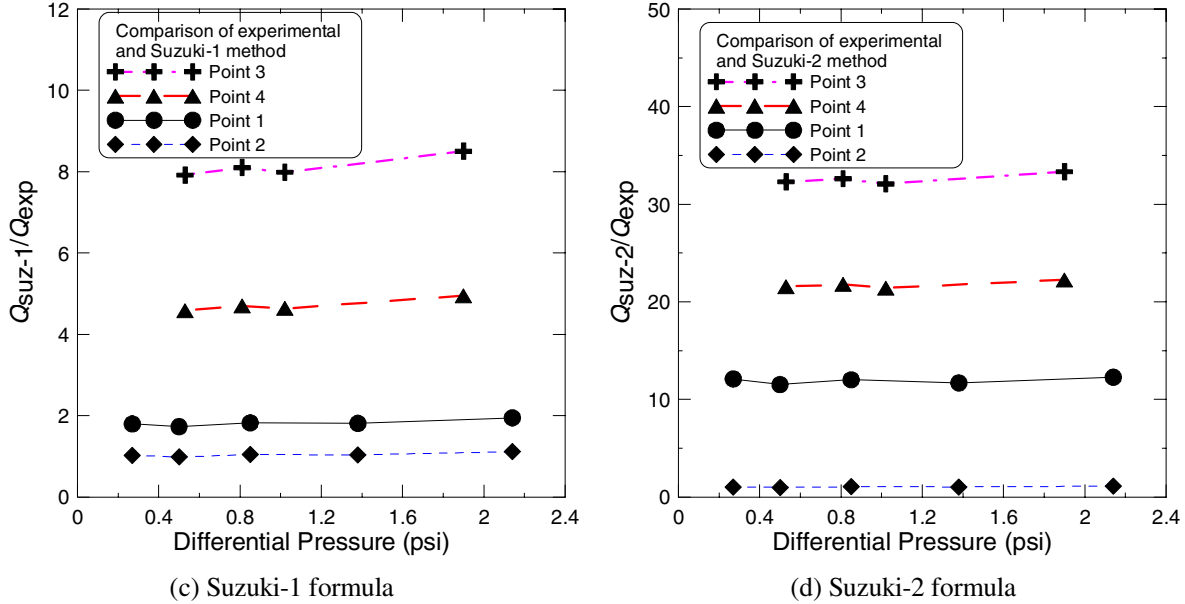


Figure 11. Comparison of experimental and analytical results of flow rate prediction (continued).

### PREDICTION OF FLOW RATE BEYOND THE NORMAL DESIGN BASIS

Using the developed finite element model and the verified leakage rate estimation formula, the flow rate of gas may be analytically predicted at larger than design basis loading. Figure 12 shows the global response of the same specimen subjected to the external lateral force  $V$  beyond its normal design basis  $\phi V_n$ . The relations between normalized predicted flow rates and the drift ratio and the ratio of external force to the  $\phi V_n$  ( $V/\phi V_n$ ) are shown in Figure 13(a) and (b). In these two plots, predicted flow rates using Suzuki-1's formula are normalized by the value predicted at  $V=\phi V_n$ . It can be observed from Figure 13(a) that the flow rate is almost zero when the drift ratio is less than 0.005%, and dramatically increases beyond a drift ratio larger than 0.015%. At larger pressure gradients, the more rapid the flow rate increases. From Figure 13(b), nearly zero flow rate is observed when the external load is smaller than  $0.6\phi V_n$ , which is consistent with the experimental results, that there is no substantial change for the load levels at  $0.3\phi V_n$  and  $0.5\phi V_n$  [5]. After the load reaches the normal design basis  $\phi V_n$ , the flow rate dramatically increases.

### SUMMARY REMARKS AND CONCLUSIONS

Unlined reinforced concrete (RC) shear walls are often used by the U.S. Department of Energy to house radioactive materials, thus providing a 'tertiary barrier'. Upon lateral earthquake loading, these stiff structural members are susceptible to large tensile and shear forces along their base and diagonal planes, where cracks can develop. Following an earthquake, dangerous gases (contained within the tertiary barrier) may leak into the environment through the cracks, lifting contamination to unsafe levels. The gas leakage rate through the damaged wall is therefore of primary concern.

To address this concern, in the presented paper, a simple methodology for analytically predicting the leakage rate of gas through RC shear walls, when subjected to a broad range of lateral demands up to and beyond their normal design basis is described. The methodology relies upon relating damage to lateral load or drift and relating gas leakage rate to damage, using finite element modeling and companion experimental studies for validation. The strain field of the specimen of interest is obtained from the finite

element analysis, and then is used to simulate the crack pattern. Flow rate estimation formulas suitable for the conditions of interest are then selected and used in conjunction with the predicted crack details to estimate flow rate at different load levels. Among the four formulas used in the present research, the method presented by Suzuki [15] provides the best estimate under the conditions of interest in this program. Furthermore, it is found that methods that do not incorporate friction between the gas flow and cracked surface (such as that by Nagano [8]), drastically overestimated the flow rate through the RC specimen. Using the developed numerical model, the relation between the gas leakage rate and shear wall lateral drift ratio or normalized lateral load, considering demands up to and beyond the design basis, is established numerically.

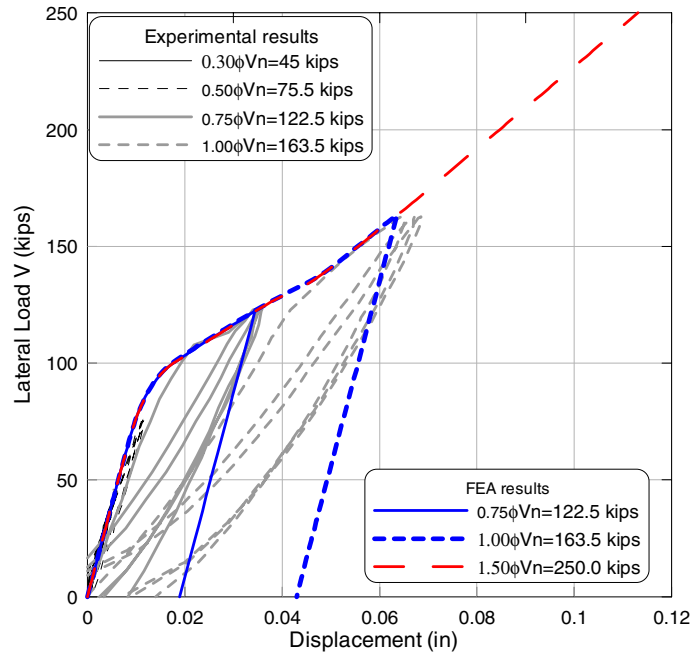


Figure 12. Comparison of experimental and finite element results.

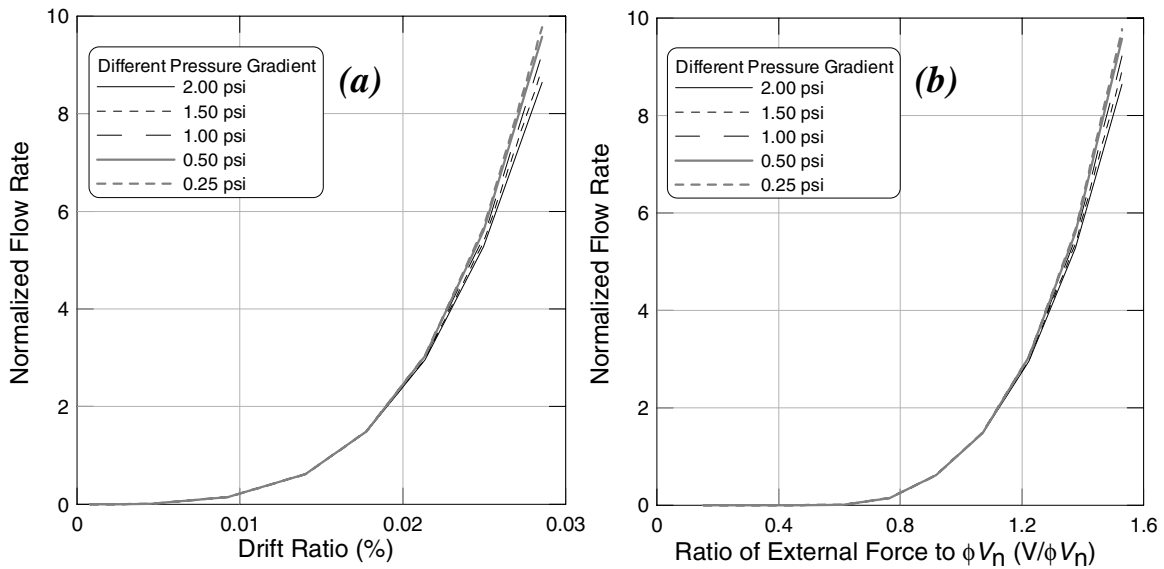


Figure 13. Normalized flow rate  $[Q_{\text{Suz-1}}/Q_{\text{Suz-1(at } V=\phi V_n)}]$  versus: (a) drift ratio (%) and (b) the ratio of applied external force to  $\phi V_n$  (i.e.  $V/\phi V_n$ ).

## ACKNOWLEDGEMENTS

The Henry Samueli School of Engineering Alumni Scholarship has provided partial support for the first author. The experimental program is supported through funding provided by Los Alamos National Laboratory. The above support is greatly appreciated.

## REFERENCES

1. Buss W. "Proof of Leakage Rate of a Concrete Reactor Building." Concrete for nuclear reactors *ACI Special Publication SP-34*, 1972, Vol. III, Paper no. 3461, 1291-1320.
2. Echeverria A, Mohraz B, Schnobrich WC, "Crack Development in a Prestressed Concrete Reactor Vessel as Determined by a Lumped Parameter Method." *Nuclear Engineering and Design*; 1970, Vol. 11, 286-294.
3. Girrens SP, Farrar CR. "Experimental Assessment of Air Permeability in a Concrete Shear Wall Subjected to Simulated Seismic Loading." Los Alamos National Laboratory Report, LA-12124-MS, Los Alamos, New Mexico. 1991.
4. Greiner U, Ramm W. "Air Leakage Characteristics in Cracked Concrete." *Nuclear Engineering and Design*, 1995, Vol. 156, 67-172.
5. Hamilton CH, Hutchinson TC, Pardoen GC, Salmon MW, Wang T. "Gas and Aerosol Leakage Rate Through Reinforced Concrete Shear Walls: Experimental Study." In the *Proceedings of the 13th World Conference on Earthquake Engineering*. Vancouver, B.C., Canada. 2004 Paper No. 2484.
6. Mayrhofer C, Korner W, Brugger W. "Gas Impermeability of Reinforced Concrete Slabs Supported on Four Sides." Part 2, Foreign Technology Division Wright-Patterson AFB report FTD-ID(RS) T-0085-88, 1988.
7. MSC.Marc. *Users Guide: Volume A-E*. MSC Software Corporation. 2001.
8. Nagano T, Kowada A, Matumura T, Inada Y, Yajima K. "Experimental Study of Leakage through Residual Shear Cracks on R/C Walls." In the *Proceedings of SMIRT-10*, 1989, Session Q, 139-144.
9. Ngo D, Scordelis AC. "Finite element analysis of reinforced concrete beams." *Journal of the American Concrete Institute*, 1967, Vol.64, No.3, Mar, 153-163.
10. Okamoto K, Hayakawa S, Kamimura R. "Experimental Study of Air Leakage from Cracks in Reinforced Concrete Walls." *Nuclear Engineering and Design*, 1995, Vol.156, 159-165.
11. Rashid YR. "Analysis of Prestressed Concrete Pressure Vessels." *Nuclear Engineering and Design*, 1968, Vol. 7, No. 4, April, 334-344
12. Riva P, Brusa L, Contri P, Imperato L. "Prediction of Air and Steam Leak Rate through Cracked Reinforced Concrete Panels." *Nuclear Engineering and Design*, 1999, Vol. 192, 13-30.
13. Rizkalla SH, Lau BL, Simmonds SH. "Air Leakage Characteristics in Reinforced Concrete." *ASCE Journal of Structural Engineering*, 1984, Vol. 110 (5), 1149-1162.
14. Suzuki T, Takiguchi K, Hotta H, Kojima N, Fukuhara M, Kimura K. "Experimental Study on the Leakage of Gas through Cracked Concrete Walls." In the *Proceedings of SMIRT-10*, 1989, Session Q, 145-150.
15. Suzuki T, Takiguchi K, Hotta H. "Leakage of Gas through Cracked Concrete Walls." *Nuclear Engineering and Design*, 1992, Vol. 133, 121-130.
16. Tinkler J, Del Frate R, Rizkalla SH. "The Prediction of Air Leakage Rate through Cracks in Pressurized Reinforced Concrete Containment Vessels." In the *Proceedings of SMIRT-8*, 1987, Session J, 25-30.